



Conductance and noise signatures of Majorana backscattering

Suk Bum Chung,¹ Xiao-Liang Qi,^{1,2} Joseph Maciejko,¹ and Shou-Cheng Zhang¹

¹*Department of Physics, Stanford University, Stanford, California 94305, USA*

²*Microsoft Research, Station Q, Elings Hall, University of California, Santa Barbara, California 93106, USA*

(Received 24 February 2011; published 23 March 2011)

We propose a conductance measurement to detect the backscattering of chiral Majorana edge states. Because normal and Andreev processes have equal probability for backscattering of a single chiral Majorana edge state, there is qualitative difference from backscattering of a chiral Dirac edge state, giving rise to half-integer Hall conductivity and decoupling of fluctuation in incoming and outgoing modes. The latter can be detected through thermal noise measurement. These experimental signatures of Majorana fermions are robust at finite temperature and do not require the size of the backscattering region to be mesoscopic.

DOI: [10.1103/PhysRevB.83.100512](https://doi.org/10.1103/PhysRevB.83.100512)

PACS number(s): 74.45.+c, 71.10.Pm, 03.67.Lx, 73.40.-c

From particle physics to condensed-matter physics, Majorana fermions currently arouse great interest.¹ In particle physics, where the concept first originated,² the experimental signature of Majorana fermions, though not yet detected, has been known for a long time, that is, the neutrinoless double β decay in the case of neutrinos.

In condensed-matter physics, two-dimensional (2D) systems where Majorana fermions can arise have been attracting a great deal of attention recently, partly due to potential applications to topological quantum computation.³⁻⁸ One class of systems where Majorana fermions can appear is the 2D chiral superconductor which has a full pairing gap in the bulk, and \mathcal{N} gapless chiral 1D Majorana fermions^{4,9} at the edge. This system can be considered as the superconducting analog of the quantum Hall (QH) state with \mathcal{N} gapless chiral edge states and is called a topological superconductor (TSC).¹⁰

The challenge now is to find a way to detect the Majorana nature of the 1D edge state in this class of systems. There has been no experiment so far which explicitly shows the Majorana nature of gapless states at the boundary of a TSC, though methods of detection have been proposed recently.^{11,12} The first issue is to find a physical system which unequivocally belongs to this class. Despite theoretical prediction that the superconducting phase of Sr_2RuO_4 is the spinful version of the $\mathcal{N} = 1$ chiral TSC due to its $p_x + ip_y$ pairing,¹³ attempts to detect the gapless edge states have not been successful.¹⁴ Therefore, we base our discussion on a recent proposal to induce topological superconductivity through the proximity effect on a magnetically doped Bi_2Se_3 film.¹⁵ The second issue is to devise an experiment that can work at reasonable temperatures, as interference effects get washed out above the temperature scale set by the size of the TSC region.¹⁶⁻¹⁸ Our approach makes use of a generalization of the Landauer-Büttiker formalism¹⁹ to superconducting systems,²⁰ which was recently used in a proposal for detecting a zero-dimensional Majorana bound state.²¹

In this Rapid Communication, we study the backscattering of the edge state of a quantum anomalous Hall (QAH) system off a $\mathcal{N} = 1$ TSC island. We find a strikingly different behavior in both conductance and noise depending on the topological invariant \mathcal{N} of the TSC, which is equal to the number of chiral Majorana edge states. In particular, for strong backscattering by the $\mathcal{N} = 1$ TSC, the incoming and outgoing channels

in the leads decouple as the probabilities for normal and Andreev scattering become equal. Indeed, whereas Andreev processes do not play any role in the case of the normal, topologically trivial superconductor (NSC) or the $\mathcal{N} = 2$ TSC, backscattering due to the $\mathcal{N} = 1$ TSC imposes a special condition between the probabilities for normal and Andreev scattering. Andreev scattering in the case of the $\mathcal{N} = 1$ TSC is due to the single chiral Dirac edge state of the QAH state splitting into *two* chiral Majorana edge states.

We first discuss how to obtain a $\mathcal{N} = 1$ TSC. When Cr or Fe magnetic dopants are introduced into Bi_2Se_3 or Bi_2Te_3 thin films, the spin exchange interaction leads to the effective Hamiltonian near the Fermi level,²²

$$h_{\text{QAH}} = \begin{pmatrix} m + Bp^2 & A(p_x - ip_y) \\ A(p_x + ip_y) & -m - Bp^2 \end{pmatrix},$$

where the basis is $(c_{\mathbf{p}\uparrow}, c_{\mathbf{p}\downarrow})^T$ with $c_{\mathbf{p}\sigma}$ annihilating an electron of momentum \mathbf{p} and spin $\sigma = \uparrow, \downarrow$ and the QAH effect obtained when $m < 0$. When this system is in proximity to an *s*-wave superconductor, the combination of Cooper pair formation through proximity effect and the electron-electron interaction gives us a nonzero pairing gap function.²³ This gives us the Bogoliubov-de Gennes (BdG) Hamiltonian

$$h_{\text{BdG}} = \begin{pmatrix} h_{\text{QAH}}(\mathbf{p}) - \mu & i\Delta\sigma^y \\ -i\Delta^*\sigma^y & -h_{\text{QAH}}^*(-\mathbf{p}) + \mu \end{pmatrix},$$

the basis for which is $(c_{\mathbf{p}\uparrow}, c_{\mathbf{p}\downarrow}, c_{-\mathbf{p}\uparrow}^\dagger, c_{-\mathbf{p}\downarrow}^\dagger)^T$. The BdG Hamiltonian can be written in a simple form for $\mu = 0$,

$$h_{\text{BdG}} = \begin{pmatrix} h_+(\mathbf{p}) & 0 \\ 0 & -h_-^*(-\mathbf{p}) \end{pmatrix}, \quad (1)$$

where

$$h_\pm(\mathbf{p}) = \begin{pmatrix} m \pm |\Delta| + Bp^2 & A(p_x - ip_y) \\ A(p_x + ip_y) & -m \mp |\Delta| - Bp^2 \end{pmatrix}, \quad (2)$$

if we use the basis $\frac{1}{\sqrt{2}}(c_{\mathbf{p}\uparrow} + c_{-\mathbf{p}\downarrow}^\dagger, c_{\mathbf{p}\downarrow} + c_{-\mathbf{p}\uparrow}^\dagger, -c_{\mathbf{p}\uparrow} + c_{-\mathbf{p}\downarrow}^\dagger, -c_{\mathbf{p}\downarrow} + c_{-\mathbf{p}\uparrow}^\dagger)^T$. The existence of Majorana edge states due to h_\pm depends entirely on the sign of $m \pm |\Delta|$,^{4,15,24} as Eq. (2) is identical to the Hamiltonian of a $p_x + ip_y$ superconductor.⁴ Thus, $|\Delta| < -m$ gives two chiral Majorana

edge states, $|\Delta| > |m|$ a single chiral Majorana edge state, and $|\Delta| < m$ no edge states. For general μ , the condition reads¹⁵

$$\begin{aligned} m < -\sqrt{|\Delta|^2 + \mu^2} &\Rightarrow \mathcal{N} = 2, \\ m^2 < |\Delta|^2 + \mu^2 &\Rightarrow \mathcal{N} = 1, \\ m > \sqrt{|\Delta|^2 + \mu^2} &\Rightarrow \mathcal{N} = 0, \end{aligned} \quad (3)$$

as the bulk gap closes only at boundaries between these three cases. These conditions show that opening up an infinitesimal SC gap gives us the $\mathcal{N} = 2$ TSC if the normal state is in the QAH phase, but it gives us the $\mathcal{N} = 1$ TSC if the normal state is a metal ($|\mu| > |m|$) obtained from doping the QAH system. This doping can come from the Fermi level mismatch between the QAH insulator and the SC used to induce the proximity effect. In the following we consider a QAH bar in proximity with a SC island in the middle, as shown in Fig. 1. The SC island can have different topological invariant determined by

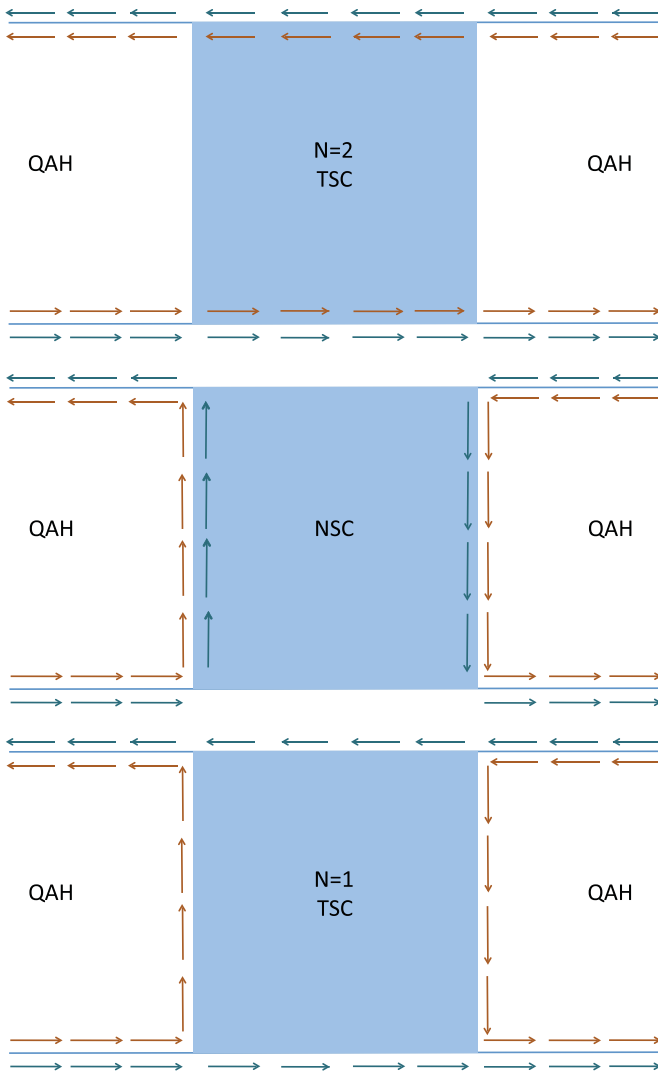


FIG. 1. (Color online) Comparison between different SCs. There is no backscattering for $\mathcal{N} = 2$ TSC, Dirac fermion backscattering for NSC, and Majorana fermion backscattering for $\mathcal{N} = 1$ TSC. Red (gray) and blue (dark gray) arrows represent $e \pm h$ chiral Majorana edge states, respectively.

Eq. (3). Here we only consider the cases where the SC island is in a uniform topological phase.

The effect of the SC island on the edge state is determined by the topological invariant of the SC island. We first note that, on the basis of Eqs. (1) and (2), the QAH edge state can be considered as two identical copies of chiral Majorana fermions, one from the upper block of Eq. (1) being $e + h$ and the other from the lower block being $e - h$,^{8,15} where e and h denote particle and hole states, respectively. In this sense, the $\mathcal{N} = 2$ TSC is topologically equivalent to the QAH insulator, and at the boundary between these two phases there will be no chiral state, as there is no change in the signs of the gaps in both h_{\pm} terms. Therefore, if we have the $\mathcal{N} = 2$ TSC for the SC island (the top of Fig. 1), the edge current will be perfectly transmitted. By contrast, the NSC is by definition topologically trivial and supports no edge states. This also implies that there will be a chiral edge state at the boundary between the QAH region and the NSC. Therefore, if we have NSC for the SC island (the middle of Fig. 1), there will be complete backscattering. In both cases, the edge state will not be involved in any violation of particle number conservation despite the presence of the SC island. In the case of the $\mathcal{N} = 1$ TSC with $\mu = 0$, we can see from Eqs. (1) and (2) that, as $|\Delta| > |m|$, the single chiral Majorana edge state comes from h_{-} . However, this also implies that at the boundary between a $\mathcal{N} = 1$ TSC and the QAH region, $m + |\Delta|$ (the gap of h_{+}) should change sign, meaning that there is a chiral Majorana state at this boundary.^{4,24} Therefore, when the $\mathcal{N} = 1$ TSC region is inserted in the middle of a QAH bar (the bottom of Fig. 1), the chiral edge state of the QAH region splits into two well-separated chiral Majorana states, in a manner analogous to the topological insulator surface state in proximity with a ferromagnet and a SC.¹⁶ Indeed, with systems that have the same splitting, we can realize an essentially equivalent setup. The interesting point in this $\mathcal{N} = 1$ TSC setup is that while one branch of chiral Majorana fermions is perfectly transmitted, the other branch is perfectly reflected.

For this reason, in the $\mathcal{N} = 1$ TSC setup of Fig. 1 there is equal probability for normal and Andreev scattering. To show this, we need to obtain the S matrix $s_{ij;\alpha\beta}$ of the TSC region which relates the annihilation operators for incoming modes $\hat{a}_{j;\beta}$ to the annihilation operators for outgoing modes $\hat{b}_{i;\alpha}$,

$$\hat{b}_{i;\alpha} = s_{ij;\alpha\beta} \hat{a}_{j;\beta}, \quad (4)$$

where $i = 1, 2$ is the lead label and $\alpha, \beta = e, h$ is the particle/hole label, which means $\hat{a}_{i;h} = \hat{a}_{i;e}^{\dagger}, \hat{b}_{i;h} = \hat{b}_{i;e}^{\dagger}$. As the QAH edge state splits into two chiral Majorana edge states, the S matrix can be factorized into two parts,

$$\begin{pmatrix} \hat{b}_{1;e} + \hat{b}_{1;e}^{\dagger} \\ \hat{b}_{2;e} + \hat{b}_{2;e}^{\dagger} \end{pmatrix} = \begin{pmatrix} -1 & 0 \\ 0 & 1 \end{pmatrix} \begin{pmatrix} \hat{a}_{1;e} + \hat{a}_{1;e}^{\dagger} \\ \hat{a}_{2;e} + \hat{a}_{2;e}^{\dagger} \end{pmatrix} \quad (5)$$

and

$$\begin{pmatrix} \hat{b}_{1;e} - \hat{b}_{1;e}^{\dagger} \\ \hat{b}_{2;e} - \hat{b}_{2;e}^{\dagger} \end{pmatrix} = \begin{pmatrix} 0 & 1 \\ 1 & 0 \end{pmatrix} \begin{pmatrix} \hat{a}_{1;e} - \hat{a}_{1;e}^{\dagger} \\ \hat{a}_{2;e} - \hat{a}_{2;e}^{\dagger} \end{pmatrix}. \quad (6)$$

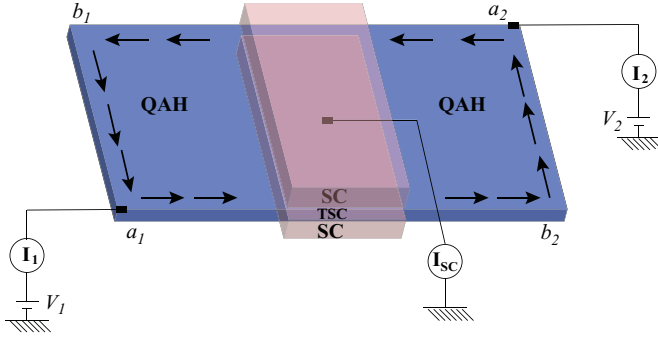


FIG. 2. (Color online) Schematic of the backscattering setup. The voltages V_1 and V_2 are applied to leads 1 and 2, respectively, and set the chemical potential for the incoming modes that are annihilated by $\hat{a}_{1,e}$ and $\hat{a}_{2,e}$. In the central region, TSC is induced through proximity to two SC slabs that sandwich the QAH. The TSC is grounded through a contact to its bulk.

This gives the S matrix

$$\begin{pmatrix} \hat{b}_{1,e} \\ \hat{b}_{1,e}^\dagger \\ \hat{b}_{2,e} \\ \hat{b}_{2,e}^\dagger \end{pmatrix} = \frac{1}{2} \begin{pmatrix} -1 & -1 & 1 & -1 \\ -1 & -1 & -1 & 1 \\ 1 & -1 & 1 & 1 \\ -1 & 1 & 1 & 1 \end{pmatrix} \begin{pmatrix} \hat{a}_{1,e} \\ \hat{a}_{1,e}^\dagger \\ \hat{a}_{2,e} \\ \hat{a}_{2,e}^\dagger \end{pmatrix}. \quad (7)$$

The elements of the first column of this S matrix correspond to the amplitudes for normal reflection, Andreev reflection, normal transmission, and Andreev transmission for the incoming right-moving particle, respectively; they are all equal up to signs. Likewise, the third column shows that these four scattering processes have equal probability for the incoming left-moving particle. The crucial point is that only when backscattering is due to the $\mathcal{N} = 1$ TSC does it involve Andreev scattering. Backscattering from the $\mathcal{N} = 2$ TSC or NSC does not involve Andreev scattering, as the splitting of the QAH chiral edge state into two chiral Majorana edge states does not happen in these cases.

Because of this property, for the $\mathcal{N} = 1$ TSC, changes of current due to the incoming modes a_1, a_2 of Fig. 2 do not lead to changes of current due to the outgoing modes b_1, b_2 . To analyze this setup using the above S matrix, we use Anantram and Datta's generalization²⁰ of the Landauer-Büttiker formalism, which allows for Andreev scattering. This formalism extends the conventional Landauer-Büttiker formula¹⁹ by adding the particle/hole index,

$$\begin{aligned} \hat{I}_i &= \frac{e}{h} \int dE \sum_{\alpha} \text{sgn}(\alpha) (\hat{a}_{i;\alpha}^\dagger \hat{a}_{i;\alpha} - \hat{b}_{j;\beta}^\dagger \hat{b}_{k;\gamma}) \\ &= \frac{e}{h} \int dE \sum_{\alpha} \sum_{jk;\beta\gamma} \text{sgn}(\alpha) A_{jk;\beta\gamma}^{(i\alpha)} \hat{a}_{j;\beta}^\dagger \hat{a}_{k;\gamma}, \end{aligned} \quad (8)$$

where $\text{sgn}(e) = 1$, $\text{sgn}(h) = -1$, and, to make Eq. (8) consistent with Eq. (4), $A^{(i\alpha)}$ is a 4×4 matrix defined as

$$A_{jk;\beta\gamma}^{(i\alpha)} \equiv \delta_{ij} \delta_{ik} \delta_{\alpha\beta} \delta_{\alpha\gamma} - s_{ij;\alpha\beta}^* s_{ik;\alpha\gamma}.$$

Just as in the Blonder-Tinkham-Klapwijk formula for the conductance of a normal-superconducting interface,²⁵ contributions from Andreev scattering cancel those of normal

scattering. This gives us the incoming currents for the leads 1 and 2,^{20,26}

$$\begin{aligned} I_1 &= \frac{e^2}{h} [(1 - \mathcal{R} + \mathcal{R}_A)(V_1 - V_{SC}) - (\mathcal{T} - \mathcal{T}_A)(V_2 - V_{SC})], \\ I_2 &= \frac{e^2}{h} [(1 - \mathcal{R} + \mathcal{R}_A)(V_2 - V_{SC}) - (\mathcal{T} - \mathcal{T}_A)(V_1 - V_{SC})], \end{aligned} \quad (9)$$

where V_{SC} is the voltage applied to the SC island, \mathcal{R}, \mathcal{T} are normal reflection and transmission probabilities and $\mathcal{R}_A, \mathcal{T}_A$ are Andreev reflection and transmission probabilities for the incoming particles.

A half-integer Hall conductivity is measured in the setup of Fig. 2 for the $\mathcal{N} = 1$ case of Fig. 1. This is because the first and the third columns of Eq. (7) give us $\mathcal{R} = \mathcal{R}_A = \mathcal{T} = \mathcal{T}_A = \frac{1}{4}$. When we ground the SC island ($V_{SC} = 0$) and apply voltage $V_1 = -V_2 = \frac{V}{2}$, Eq. (9) gives

$$I_1 = -I_2 = \frac{e^2}{2h} V,$$

which are currents flowing into leads 1 and 2, respectively. This result is due to the increase of incoming current by $e^2 V/2h$ in lead 1 and decrease of incoming current by $e^2 V/2h$ in lead 2, while outgoing current stays the same for both leads. Thus, charge is conserved in this voltage setup. In addition, the QAH edge is grounded along with the SC region and all the voltage drop occurs at the contacts to the voltage. By contrast, for the $\mathcal{N} = 2$ TSC or the NSC in the same setup, we will measure Hall conductivity of e^2/h and 0, respectively.

Whether Andreev scattering processes are involved or not can be shown directly by measuring the current flowing from the SC island to the ground. When $V_2 \neq -V_1$, the change in the right-moving current $e^2 V_1/h$ will not be canceled by the change in the left-moving current $e^2 V_2/h$. In the case of the $\mathcal{N} = 1$ TSC, however, these currents do not flow out into the outgoing modes b_1, b_2 of the QAH region. Rather, since the SC island in our setup is not floating but grounded (Fig. 2), the net incoming current,

$$I_{SC} = \frac{e^2}{h} (V_1 + V_2), \quad (10)$$

will be flowing from the SC island to the ground. On the other hand, for the NSC or the $\mathcal{N} = 2$ TSC, all incoming current will flow out into the outgoing modes b_1, b_2 of the QAH region, and no current will flow from the SC island to the ground. This will hold true regardless of whether we have $V_2 \neq -V_1$ or not. In other words, unlike for the NSC or the $\mathcal{N} = 2$ TSC, the current is not solely determined by $V_1 - V_2$ for the $\mathcal{N} = 1$ TSC.

Noise measurements will also show qualitative differences from the case of normal backscattering, because the correlation between current fluctuations in the same lead is unaffected by backscattering while the correlation between current fluctuations in different leads vanishes. From the Anantram-Datta formalism, we obtain the zero frequency noise,²⁰

$$\begin{aligned} S_{ij} &= \frac{2e^2}{h} \sum_{\alpha\beta} \sum_{kl;\gamma\delta} \int dE \text{sgn}(\alpha) \text{sgn}(\beta) A_{kl;\gamma\delta}^{(i\alpha)} A_{lk;\delta\gamma}^{(j\beta)} \\ &\quad \times n_{k\gamma} (1 - n_{l\delta}). \end{aligned}$$

This gives us the noise formula for $eV_{1,2} \ll k_B T$:

$$\begin{aligned} S_{11} = S_{22} &= \frac{4e^2}{h} k_B T (1 - \mathcal{R} + \mathcal{R}_A), \\ S_{12} &= \frac{4e^2}{h} k_B T (-\mathcal{T} + \mathcal{T}_A), \end{aligned} \quad (11)$$

which clearly gives $S_{11} = S_{22} = \frac{4e^2}{h} k_B T$ and $S_{12} = 0$. Interestingly, even if the $\mathcal{N} = 1$ TSC is near the transition to the $\mathcal{N} = 2$, so that the $e - h$ chiral Majorana state is not reflected perfectly as in Eq. (5), we would still have $\mathcal{R} = \mathcal{R}_A$ as long as Eq. (6) stays unmodified. Thus, in this case, although $S_{12} \neq -S_{ii}$, we do have $S_{11} = S_{22} = \frac{4e^2}{h} k_B T$ just like the case where the chiral edge state transmits perfectly. Similarly, near the transition between $\mathcal{N} = 1$ TSC and $\mathcal{N} = 0$ NSC, we have $S_{12} = 0$ just like the case chiral edge state reflects perfectly, though S_{11} and S_{22} are nonzero. This decoupling of the self- and cross-noise correlation is a special feature of our backscattering setup absent in previous proposals^{18,27,28} to detect the Majorana state through noise measurement.

We emphasize that the above results for the thermal noise hold only because we are keeping the chemical potential of the SC fixed by grounding it. If the SC potential is floating, that is, not connected directly to any external voltage, combination of current conservation $I_1 + I_2 = 0$ and V_{SC} fluctuation will result in the Johnson-Nyquist relation $S_{11} = S_{22} = -S_{12} = 4Gk_B T$ where G is the conductance between the two leads. Indeed, even if there is Andreev scattering, this relation should always hold for the two-terminal measurement.²⁰

These subtleties do not have any effect when backscattering is caused by the $\mathcal{N} = 2$ TSC or NSC, where $S_{11} = S_{22} = -S_{12} = 4Gk_B T$ always holds. This is because in those cases $\mathcal{R} + \mathcal{T} = 1$ and $\mathcal{T}_A = \mathcal{R}_A = 0$. For the setup of Fig. 1, we have $\mathcal{R} = 1$ for the NSC, which gives $G = 0$ and thus reduces all noise to zero. For the $\mathcal{N} = 2$ TSC, we have $\mathcal{R} = 1$ for the NSC, which gives $G = e^2/h$ and $S_{11} = S_{22} = -S_{12} = 4(e^2/h)k_B T$. Whereas for the conductance, the $\mathcal{N} = 1$ TSC gives a value that is halfway between that of the NSC and the $\mathcal{N} = 2$ TSC, for the noise, we find S_{ii} to be just that of the $\mathcal{N} = 2$ TSC and S_{12} to be that of the NSC.

In summary, we have described a method to detect a chiral Majorana state through transport measurements. Probabilities for normal and Andreev scattering are equal when backscattering occurs through a single chiral Majorana state. If the voltage is applied symmetrically ($V_2 = -V_1$), this gives a half-integer Hall conductivity, and if not, we will have a quantized current flowing from the SC to the ground [Eq. (10)]. Also, due to normal and Andreev scattering having the same probability, the correlation of current fluctuations within the same lead is unaffected by backscattering, while the correlation of current fluctuations in different leads vanishes.

We would like to thank Steve Kivelson, David Goldhaber-Gordon, Mac Beasley, Matthew Fisher, and Liang Fu for sharing their insights. This work is supported by DOE under Contract No. DE-AC02-76SF00515 (S.B.C.), the Stanford GF Program (J.M.), and NSF under Grant No. DMR-0904264.

¹F. Wilczek, *Nat. Phys.* **5**, 614 (2009).

²E. Majorana, *Nuovo Cimento* **5**, 171 (1937).

³G. Moore and N. Read, *Nucl. Phys. B* **360**, 362 (1991).

⁴N. Read and D. Green, *Phys. Rev. B* **61**, 10267 (2000).

⁵D. A. Ivanov, *Phys. Rev. Lett.* **86**, 268 (2001); A. Stern, F. von Oppen, and E. Mariani, *Phys. Rev. B* **70**, 205338 (2004); M. Stone and S. B. Chung, *ibid.* **73**, 014505 (2006).

⁶A. Kitaev, *Ann. Phys.* **321**, 2 (2006).

⁷C. Nayak, S. H. Simon, A. Stern, M. Freedman, and S. Das Sarma, *Rev. Mod. Phys.* **80**, 1083 (2008).

⁸L. Fu and C. L. Kane, *Phys. Rev. Lett.* **100**, 096407 (2008); J. D. Sau, R. M. Lutchyn, S. Tewari, and S. Das Sarma, *ibid.* **104**, 040502 (2010); Y. Tanaka, T. Yokoyama, and N. Nagaosa, *ibid.* **103**, 107002 (2009).

⁹G. E. Volovik, *Sov. Phys. JETP* **67**, 1804 (1988).

¹⁰X.-L. Qi, T. L. Hughes, S. Raghu, and S.-C. Zhang, *Phys. Rev. Lett.* **102**, 187001 (2009); R. Roy, e-print [arXiv:0803.2868](https://arxiv.org/abs/0803.2868) (to be published); A. P. Schnyder, S. Ryu, A. Furusaki, and A. W. W. Ludwig, *Phys. Rev. B* **78**, 195125 (2008).

¹¹S. B. Chung and S.-C. Zhang, *Phys. Rev. Lett.* **103**, 235301 (2009); R. Shindou, A. Furusaki, and N. Nagaosa, *Phys. Rev. B* **82**, 180505(R) (2010).

¹²L. Fu and C. L. Kane, *Phys. Rev. B* **79**, 161408 (2009).

¹³T. M. Rice and M. Sigrist, *J. Phys. Condens. Matter* **7**, L643 (1995).

¹⁴P. G. Bjornsson, Y. Maeno, M. E. Huber, and K. A. Moler, *Phys. Rev. B* **72**, 012504 (2005); J. Kirtley, C. Kallin, C. W. Hicks, E. A.

Kim, Y. Liu, K. A. Moler, Y. Maeno, and K. D. Nelson, *ibid.* **76**, 014526 (2007).

¹⁵X.-L. Qi, T. L. Hughes, and S.-C. Zhang, *Phys. Rev. B* **82**, 184516 (2010).

¹⁶L. Fu and C. L. Kane, *Phys. Rev. Lett.* **102**, 216403 (2009).

¹⁷A. R. Akhmerov, J. Nilsson, and C. W. J. Beenakker, *Phys. Rev. Lett.* **102**, 216404 (2009).

¹⁸K. T. Law, P. A. Lee, and T. K. Ng, *Phys. Rev. Lett.* **103**, 237001 (2009).

¹⁹M. Büttiker, *Phys. Rev. B* **46**, 12485 (1992).

²⁰M. P. Anantram and S. Datta, *Phys. Rev. B* **53**, 16390 (1996).

²¹J. Nilsson, A. R. Akhmerov, and C. W. J. Beenakker, *Phys. Rev. Lett.* **101**, 120403 (2008).

²²R. Yu, W. Zhang, H.-J. Zhang, S.-C. Zhang, X. Dai, and Z. Fang, *Science* **329**, 61 (2010).

²³P. G. de Gennes, *Rev. Mod. Phys.* **36**, 225 (1964).

²⁴B. A. Bernevig, T. L. Hughes, and S.-C. Zhang, *Science* **314**, 1757 (2006).

²⁵G. E. Blonder, M. Tinkham, and T. M. Klapwijk, *Phys. Rev. B* **25**, 4515 (1982).

²⁶O. Entin-Wohlman, Y. Imry, and A. Aharony, *Phys. Rev. B* **78**, 224510 (2008).

²⁷C. J. Bolech and E. Demler, *Phys. Rev. Lett.* **98**, 237002 (2007).

²⁸S. Tewari, C. Zhang, S. Das Sarma, C. Nayak, and D.-H. Lee, *Phys. Rev. Lett.* **100**, 027001 (2008).